SSRG International Journal of Electronics and Communication Engineering
ISSN: 2348-8549/ https://doi.org/10.14445/23488549/IJECE-V12I2P105

Volume 12 Issue 2, 54-64, February 2025

Original Article

Towards Reliable Wireless Communication in High Speed Trains Using Massive MIMO

Maharshi Bhatt[1], Komal Borisagar[2]

[1]*Gujarat Technological University, Ahmedabad, Gujarat, India.*
[1]*Department of E&C Engineering, Govt. Engineering College, Bhuj, Gujarat, India.*
[2]*GSET, Gujarat Technological University, Ahmedabad, Gujarat, India.*

[1]*Corresponding Author : maharshi88@gmail.com*

Received: 07 December 2024 Revised: 05 January 2025 Accepted: 06 February 2025 Published: 26 February 2025

Abstract - *Nowadays, High-Speed Train is efficiently used as the fastest mode of ground transportation. To provide Seamless high-speed wireless broadband connectivity onboard the train is a huge challenge. Major challenges in high-speed rail scenarios are Intercarrier Interference, Channel estimation errors, Doppler spread, Carrier frequency offset and Inter beam interference. Massive MIMO has been proven to be an emerging technique for high data rate communication in high mobility scenarios due to higher throughput, higher spectra, and higher energy efficiency. In this paper, various wireless channel parameters like achievable rate in bits/S/Hz for MF and MMSE receivers, Doppler spread in beamforming antenna systems, radiation beam patterns and Constellation diagrams for various modulation methods are derived. RMS value of Error Vector Magnitude (% EVM) is also derived for all users for various cases. The new advanced system with kalman filtering is proposed, and Bit Error Rate vs SNR is obtained for QPSK modulation schemes and different numbers of Tx antennas for High Speed Train. From overall simulation results, it is observed that by increasing more number of antennas in the Massive MIMO system, a high-performance wireless communication system for high-speed trains can be designed.*

Keywords - *Massive MIMO, High speed train, Signal to noise ratio, Doppler Frequency Offset, Bit error rate, Spectral efficiency, Radiation beam, Inter beam interference, Ergodic achievable rate, Error vector magnitude, Beamforming.*

1. Introduction

Massive MIMO (Multiple Input Multiple Output) systems have recently emerged as novel wireless communication technology with numerous attractive characteristics and achievable capacity that can be increased by simply installing hundreds of antennas at the Base station. High spectral efficiency can be achieved due to large multiplexing gain and antenna array gain due to more Tx antennas [1]. Energy conservation is extremely necessary in the existing scenario of the world. Massive MIMO technology reduces power consumption by generating sharp, narrow beam radiation in the direction of the user only and prevents the power of unwanted omnidirectional radiation. Thus, it achieves huge energy efficiency [2]. If any one antenna becomes non-working then also due to large number of antenna makes transmission robust. The above features of the Massive MIMO system make this technology a key role player for the 5G communication system. The extensive popularity of high-speed trains will indeed require high data rate railway communication services onboard the train at a speed of around 400 km/hr simultaneously to a large number of passengers [3]. The majority of the current wireless communication systems are designed for medium-speed travelling users. The high speed of the train limits the efficiency of a wireless communication channel. A Global Mobile For Rail (GSM-R) system is currently implemented for high-speed train communication, which supports a maximum data rate of less than 200 kbps at speeds of 300 to 350 mph [3]. Massive MIMO system architecture for High Speed Train is shown in Figure 1.

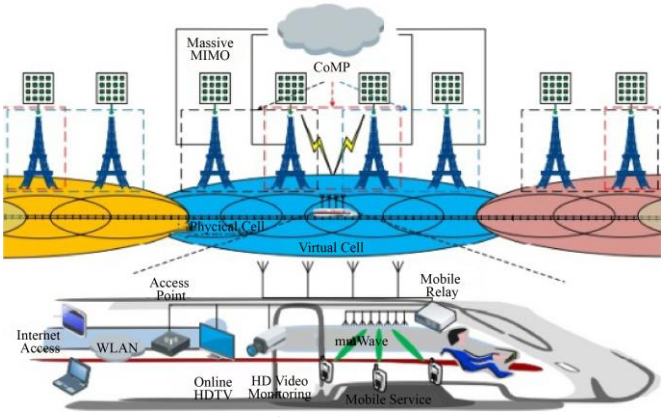

Fig. 1 Architecture of massive MIMO in HST scenario

Major challenges for High-Speed Train communication are briefly described below. As per testing records, the present 4G systems can only offer a data rate of 2 Mbps for high-speed

trains [4]. Upcoming high mobility systems are expected to give high-speed internet services to users travelling in high-speed vehicles at a very high data rate. Hence, it is necessary to evolve new technologies designed specifically for high-mobility scenarios. Significant Challenges of High Mobility wireless communications are Channel estimation errors, Doppler spread, Fast time-varying fading, Inter beam interference, Carrier frequency offset, Intercarrier interference and High penetration loss. Intercarrier interference occurs due to frequency shift due to the Doppler effect; hence, orthogonality between OFDM subcarrier vanishes. Doppler spread occurs due to relative motion between transmitter and receiver, which causes a shift in transmitted signal frequency.

In high mobility systems, channel estimation errors are unavoidable, and they will severely degrade system performance. The Doppler shift at the received signal can generate a frequency mismatch between the transmitter and receiver oscillators, called Carrier Frequency Offset (CFO). In high mobility systems with doubly selective fading, the channel changes inside one OFDM symbol, destroying the orthogonality among subcarriers and introducing ICI (Intercarrier Interference) [5]. In HSR(High-Speed Rail) systems, the well-sealed train coaches cause high penetration loss of the wireless signals.

1.1. Research Gap and Problem Definition

After a thorough literature review and analysis, the following research gap is identified in high-speed wireless communication in the high-speed mobility scenario, and the problem has been defined for work as below.

- To Analyze the effect of the number of Tx antennas on ergodic channel data rate in high-speed trains.
- To develop an algorithm to reduce inter-beam interference in massive MIMO and analyze performance by changing the number of Tx antennas for high-speed train scenarios [6].
- To Optimize a number of antennas for beamforming networks in massive MIMO to achieve lower doppler spread with different types of beamformers in HSR.
- To obtain the relation of Bit Error Rate and Signal Noise Ratio (SNR) for different modulation schemes and different numbers of Tx antennas.

This research paper is well organized, as mentioned below:

In this paper, the achievable rate by MF receiver and MMSE receiver is derived from w.r.t number of BS antennas and compared to the results in Section 2. Multiple parallel beamforming branches of a massive MIMO antenna are introduced to compensate for the Doppler Frequency Offset in Section 3. The radiation pattern of massive MIMO beamforming antennas is derived, and a constellation diagram is also derived for various parameters, as shown in Section 4. The new proposed system model of Massive MIMO using Kalman filter for channel estimation is designed and shown in Section 5. BER performance is analyzed for different speeds of high-speed trains and different values of SNR. Validation of the results was carried out in Section 6. The conclusion and future research scope is mentioned in Section 7.

2. Effect on Achievable Rate by Massive MIMO

The achievable data rate in the uplink wireless channel depends on the number of base station antennas. Here, for the MF (Matched Filter) and MMSE (Minimum Mean Square Error) receiver, SNR is derived and based on SNR, the achievable rate in bits/sec/Hz is derived.

The following parameters are considered for mathematical analysis and simulation.

Mathematical analysis:

1. Number of user = 10
2. ICI (inter-cell interference) $\alpha = 0.1$
3. Cells within a cluster $L = 3$
4. Degree of Freedom DoF, $P = N$
5. Effective training SNR ptr = 6 dB
6. Transmit signal SNR p= 10 dB

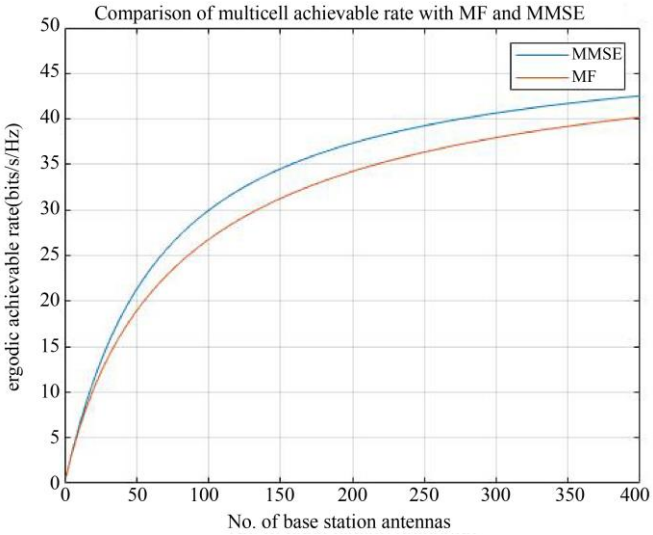

Fig. 2 Comparison of achievable rate Vs. No. of BS antenna for MF reveiver and MMSE receiver

2.1. Observation from Simulation

- In plots, ergodic achievable rate versus no. of base station antennas for MF (Matched Filter) detection and MMSE (Minimum Mean Square Error) detection is obtained.
- It shows that as the number of antennae increases, the achievable rate also increases, and accordingly, we can select how many antennas are required to achieve the required achievable rate.
- In Figure 2, comparing the achievable rate with MF and MMSE detection, we can observe that using the same number of base station antennas can achieve a higher ergodic achievable rate with MMSE detection than with MF detection.

- Hence, it is observed that the MMSE detector is better due to its high immunity to interference and its better achievable rate compared to the MF detector.

3. Optimization of no. of Antennas for Beamforming NW in Massive MIMO to Achieve Lower Doppler Spread

It is observed generally in wireless fading channels that the channel time variation can be effectively suppressed if the signal is transmitted by a huge number of Transmit antennas. In designing a beamforming network to generate multiple parallel beamforming branches, each individual branch will transmit a signal to one particular angle. Due to this, a single dominant DFO (Doppler Frequency Offset) will affect the transmitted signal, which can be easily compensated before transmission of the signal. As per the scaling law of channel variation, It is defined that the Doppler spread is proportional to the maximum DFO and decreases inversely proportional to $\sqrt{M}$ (*M is the number of transmit antennas)*[7].

3.1. Compensation of Doppler Spread by Massive MIMO

The received signal at each antenna will face multiple DFOs. Since the DFOs are related to the Angle of Departure, it is challenging to separate them with a single antenna. We can simultaneously design multiple parallel beamforming branches, as shown in Figure 3. By this technique, each branch transmits a signal towards the pre-determined direction through a high-resolution beamforming network [7]. As the transmitted signal in each branch is accommodated within a narrow beam, it is primarily affected by a single DFO when propagating over the channel. Therefore, it is possible to design a single DFO compensation at the transmitter for each branch.

3.2. Mathematical Analysis of Doppler Spread

The Doppler spread σ is proportional to the maximum DFO f_d, and when no. of Tx antennas M is sufficiently large, σ can be approximated as [7].

$$\sigma \simeq 2\pi\kappa\, f_d\, (\ln(4M))^{-1/2}\, M^{-1/2} \qquad (1)$$

Where
σ = *Doppler spread*
κ = *coefficient*
f_d = *maximum DFO* = v/λ (v = *velocity of moving object* , λ = *wavelength of signal)*
M = *No. of Tx antenna*

For parameter values given in Table 1, we get the plot of the Doppler spread for different values of Tx antennas.

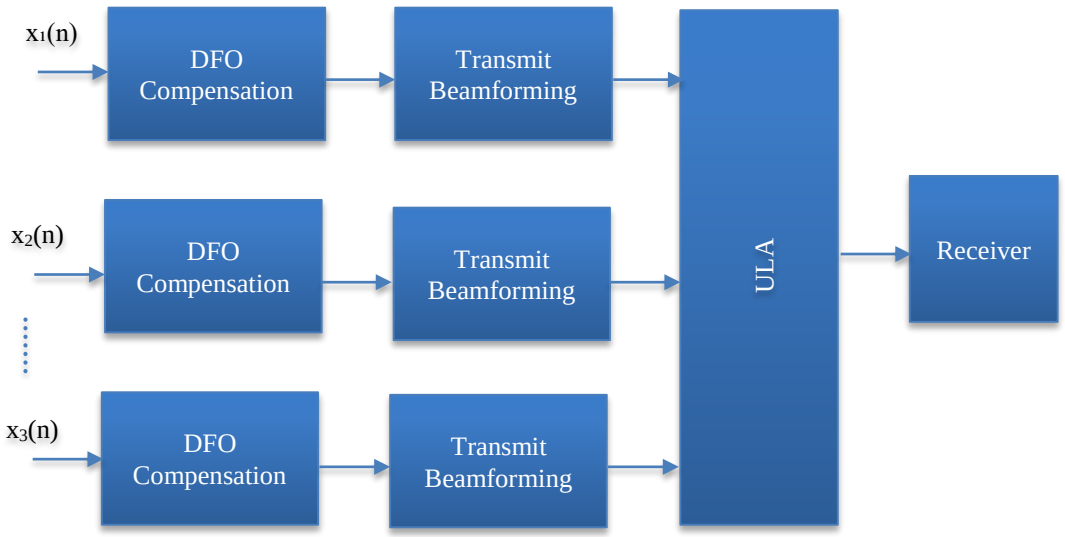

Fig. 3 Transmitter design for Doppler Frequency (DFO) compensation

3.3. Iteration 1

Table 1. Parameters values for iteration 1

S No.	Parameters	Value
1	Velocity of HSR, v	360 km/h
2	Wavelength of signal, λ	0.1 m
3	Carrier frequency	3 GHz
4	Coefficient, k	0.7
5	Maximum DFO, fd	1000 Hz

3.4. Iteration 2

Table 2. Parameters values for iteration 2

S No.	Parameters	Value
1	Velocity of HSR, v	400 km/h
2	Wavelength of signal, λ	0.1 m
3	Carrier frequency	3 GHz
4	Coefficient, k	0.7
5	Maximum DFO, fd	1111 Hz

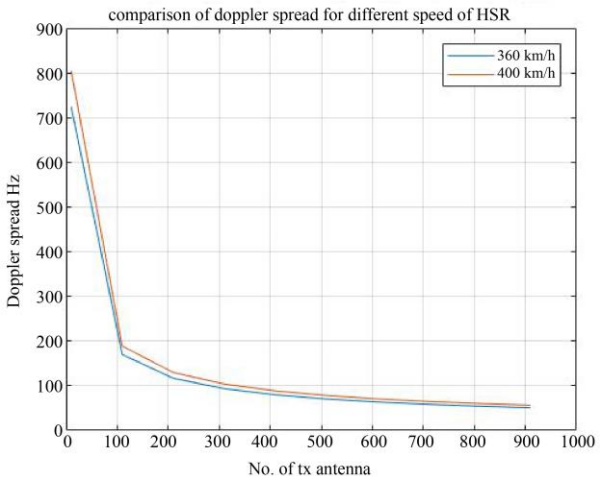

Fig. 4 Plot of comparison of doppler spread for different speeds of HSR

Table 3. Comparison of doppler spread for 360 Km/H speed & 400 Km/H speed of train (Nt Is No. Of Tx antenna)

Parameters	Case -1	Case -2
Velocity of HSR, v	360 km/h	400 km/h
Wavelength of signal, λ	0.1 m	0.1 m
Co-efiicient, k	0.7	0.7
Maximum DFO, fd	1000 Hz	1111 Hz
Doppler spread for Nt = 50	500 Hz	600 Hz
Doppler spread for Nt = 200	110 Hz	130 Hz
Doppler spread for Nt = 500	80 Hz	90 Hz

3.5. Observation from Results

By generating multiple parallel beamforming branches, the transmitted signal will experience only dominant Doppler Frequency Offset (DFO). To design such a transmission network, we need more number of BS antennae to form multiple parallel beamforming branches. As shown in Tables 1 and 2, by increasing more number of BS antennas, Doppler spread is decreased. Iteration 1 is derived from the 360 km/hr velocity of a high-speed train, while iteration 2 is derived from the 400 km/hr velocity. From Figure 4, it is observed that as the velocity of HSR increases, Doppler spread also increases for the same number of Tx antennas.

4. Radiation Pattern of Massive MIMO Beamforming Antenna NW and Analysis

Massive MIMO systems have been accepted as the main technique for 5G wireless communications. In terms of power usage, it is not affordable to allocate one Radio Frequency (RF) chain to each antenna in a massive MIMO. So, hybrid analog and digital beamforming decreases the number of RF chains [8].

The objective of Massive MIMO beamforming is to form beams that can be shared by multiple users, allowing simultaneous data transmission while minimizing interference [9]. The beams formed by adjusting the phase and amplitude of the signals sent from multiple antennas are simultaneously transmitted to the intended users [10].

In scattering channel type and 256-point FFT OFDM channel modulation, the radiation pattern of Massive MIMO is obtained for different numbers of BS antennas and different numbers of user antennas. In this simulation, a convolution channel encoder is used. The cyclic prefix length of the OFDM block is 64-bit [11]. A constellation diagram for various signal modulation schemes is also derived for each iteration. For each iteration, a percentage RMS Error Vector Magnitude (EVM) is obtained for each user.

- A constellation diagram is a visual representation of a modulation scheme. It illustrates the possible signal states in a two-dimensional space, showing the amplitude and phase of each symbol.
- Each point on the diagram represents a unique symbol or signal state in the modulation scheme.
- The distance between points represents how easily symbols can be distinguished from one another. Larger distances provide better noise immunity but may reduce the efficiency of bandwidth usage.

The error vector is the difference (in magnitude and phase) between the ideal point and the actual received point for a given symbol. EVM calculates the RMS (Root Mean Square) of these error vectors over a set of symbols to quantify the average deviation. A lower EVM percentage indicates higher signal quality and better system performance. High EVM values suggest significant degradation due to noise, distortion, or hardware imperfections.

4.1. Iteration -1

Table 4. Parameter values for iteration 1

S No.	Parameter	Value
1	No. of BS Tx antenna	64
2	No. of users considered	4
3	No. of data stream per user	[3 2 1 2]
4	No. of Rx antenna per user	16
5	Signal Modulation scheme	16 QAM
6	Signal carrier frequency	28 GHz
7	Channel type	Scattering
8	Noise figure of channel	8 dB
9	Channel modulation	OFDM (256 point FFT)
10	Channel encoder	Convolution encoder

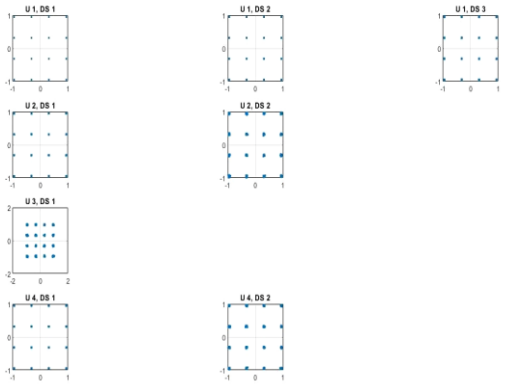

Fig. 5 Constellation diagram for 16 QAM

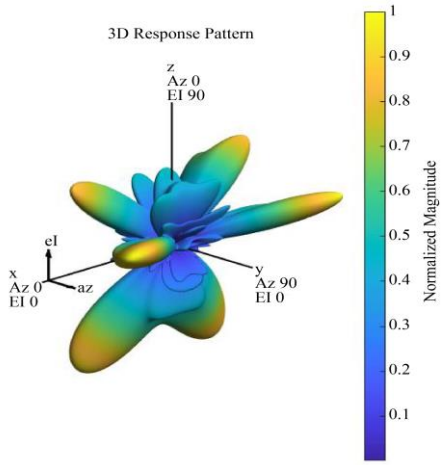

Fig. 6 Radiation pattern of massive MIMO beamforming antenna for iteration 1

- User 1
  RMS EVM (%) = 0.38361
- User 2
  RMS EVM (%) = 1.0311
- User 3
  RMS EVM (%) = 2.1462
- User 4
  RMS EVM (%) = 1.0024

4.2. Iteration -2

Table 5. Parameter values for iteration 2

S No.	Parameter	Value
1	No. of BS Tx antenna	64
2	No. of users considered	4
3	No. of data stream per user	[3 2 1 2]
4	No. of Rx antenna per user	16
5	Signal Modulation scheme	64 QAM
6	Signal carrier frequency	28 GHz
7	Channel type	Scattering
8	Noise figure of channel	8 dB
9	Channel modulation	OFDM (256 point FFT)
10	Channel encoder	Convolution encoder

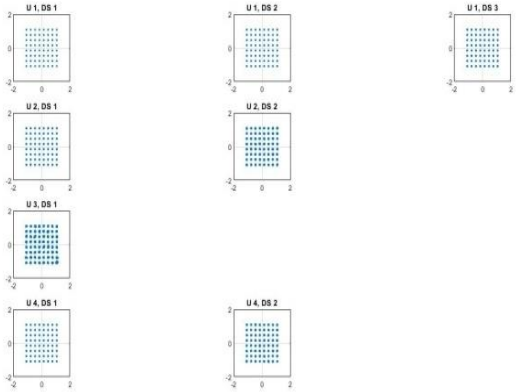

Fig. 7 Constellation diagram for 64 QAM

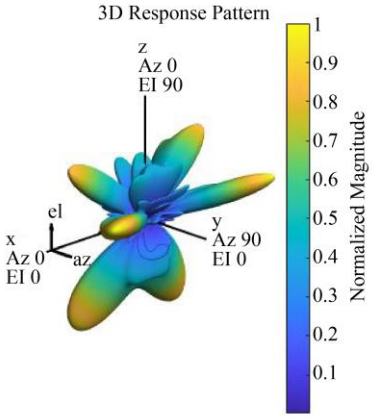

Fig. 8 Radiation pattern of massive MIMO beamforming antenna for iteration 2

- User 1
  RMS EVM (%) = 0.37937
- User 2
  RMS EVM (%) = 1.1777
- User 3
  RMS EVM (%) = 2.1031
- User 4
  RMS EVM (%) = 0.98249

4.3. Iteration-3

Table 6. Parameter values for iteration 3

S No.	Parameter	Value
1	No. of BS Tx antenna	128
2	No. of users considered	4
3	No. of data stream per user	[3 2 1 2]
4	No. of Rx antenna per user	16
5	Signal Modulation scheme	64 QAM
6	Signal carrier frequency	28 GHz
7	Channel type	Scattering
8	Noise figure of channel	8 dB
9	Channel modulation	OFDM (256 point FFT)
10	Channel encoder	Convolution encoder

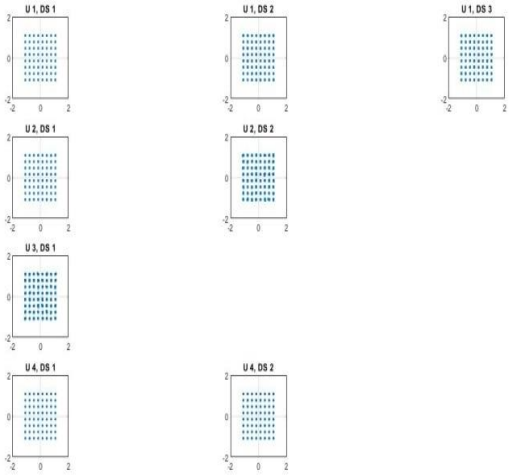

Fig. 9 Constellation diagram for 64 QAM

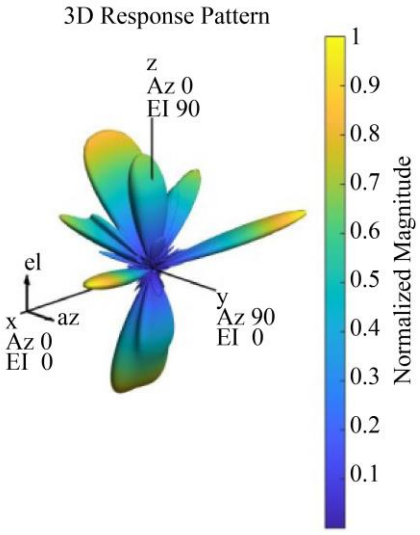

Fig. 10 Radiation pattern of massive MIMO beamforming antenna for iteration 3

- User 1
  RMS EVM (%) = 0.8482
- User 2
  RMS EVM (%) = 1.1042
- User 3
  RMS EVM (%) = 1.4424
- User 4
  RMS EVM (%) = 0.55672

4.4. Iteration-4

Table 7. Parameter values for iteration 4

S No.	Parameter	Value
1	No. of BS Tx antenna	256
2	No. of users considered	4
3	No. of data stream per user	[3 2 1 2]
4	No. of Rx antenna per user	16
5	Signal Modulation scheme	16 QAM
6	Signal carrier frequency	28 GHz
7	Channel type	Scattering
8	Noise figure of channel	8 dB
9	Channel modulation	OFDM (256 point FFT)
10	Channel encoder	Convolution encoder

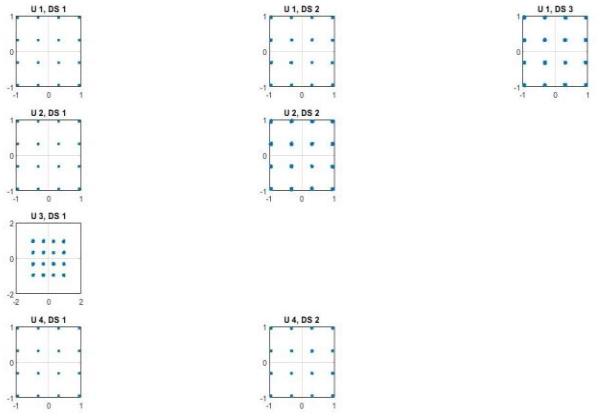

Fig. 11 Constellation diagram for 16 QAM

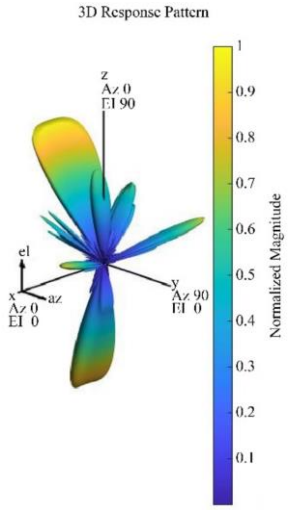

Fig. 12 Radiation pattern of massive MIMO beamforming antenna for iteration

- User 1
  RMS EVM (%) = 1.0486
- User 2
  RMS EVM (%) = 1.0577
- User 3
  RMS EVM (%) = 2.0186
- User 4
  RMS EVM (%) = 0.63687

4.5. Result Analysis and Observation

Table 8. Comparison of EVM (%) for different BS antennas and modulation scheme

Iteration	No. of BS antennas	Modulation scheme	No. of Rx antenna per user	User 1 EVM (%) (DS 3)	User 2 EVM (%) (DS 2)	User 3 EVM (%) (DS1)	User 4 EVM (%) (DS 2
1	64	16 QAM	16	0.38361	1.0311	2.1462	1.0024
2	64	64 QAM	16	0.37937	1.1777	2.1031	0.98249
3	128	64 QAM	16	0.8482	1.1042	1.4424	0.55672
4	256	16 QAM	16	1.0486	1.0577	2.0186	0.63687

In each iteration, highlighted parameters in the respective table are changed, and the beamforming network's corresponding constellation diagram and radiation pattern are derived. The following findings are observed from the constellation diagram and radiation pattern.

- As we increase the number of BS antennas from 64 to 128 , EVM (%) decreases, but if the data stream per user is 3 or more, EVM (%) increases.
- As we increase the number of BS antennas, constellation points are less scattered (Figures 9 and 11) and are well centered. It means that SNR is increased.
- From the radiation pattern, it is observed that if we increase the number of BS antennae, the radiation beam for the user becomes sharp and narrow (Figures 10 and 12). So, inter-beam interference is reduced.
- As the radiation beam for the user is narrower, energy efficiency is higher because lower power is required for a narrow beam compared to a wide radiation beam.
- Due to the narrow beam, we can assign the same time-frequency resources to each user, as there is no possibility of inter-beam interference.
- In this way, it is concluded that by increasing number of BS antennae in the Massive MIMO beam-forming antenna network, as shown in Table 8, we can achieve higher spectral efficiency and higher energy efficiency.

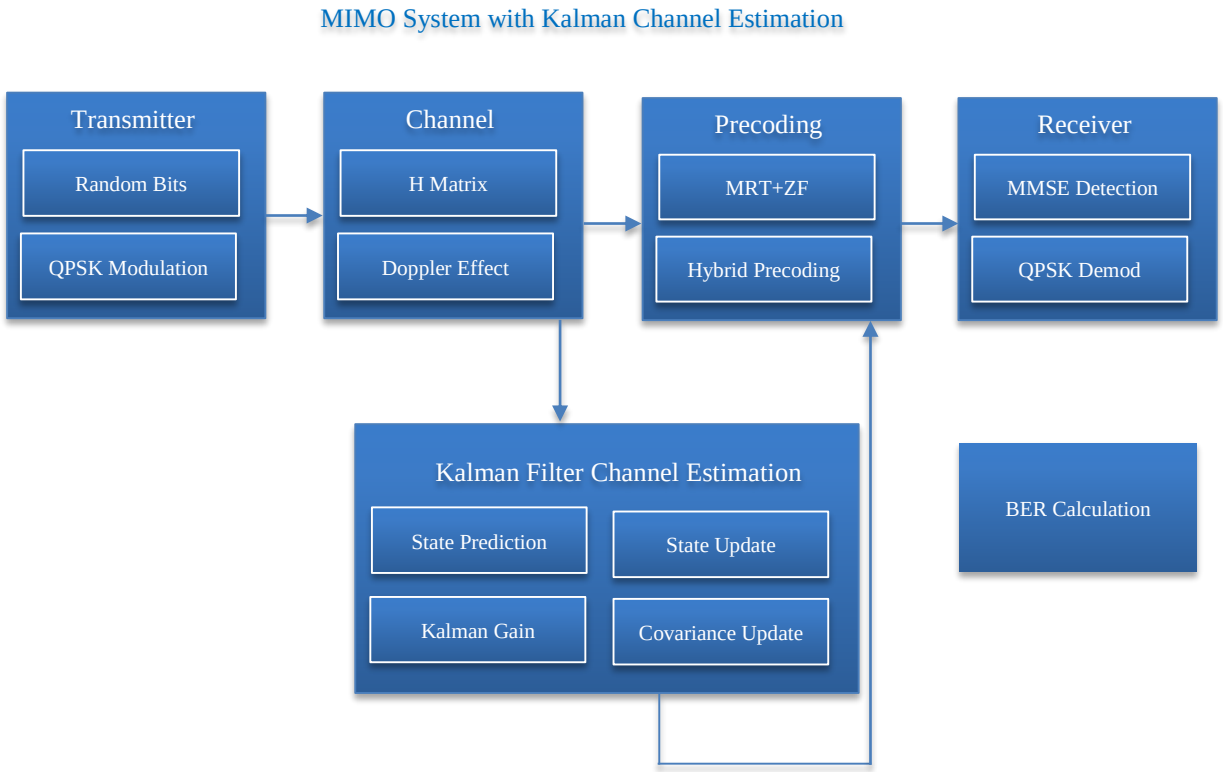

Fig. 13 Block diagram of proposed advanced method to reduce BER of the system for HST scenario

5. Bit Error Rate (BER) Performance Analysis of the Proposed System with Kalman Filter for High-Speed Train Scenario

To achieve reliable BER performance in high-speed train scenarios, the following techniques are proposed in the Massive MIMO system.

- More number of antennas are used at Tx and Rx.
- A lower modulation order is used for more reliability.
- An advanced channel estimation method (Kalman filtering) is used. Kalman filtering is a recursive algorithm that estimates the state of a system from noisy measurements.
- A hybrid precoding strategy is used. Combines MRT (Maximum Ratio Transmission) and ZF precoding together to maintain interference suppression.
- Optimal antenna selection based on channel gain.
- MMSE detection with noise variance optimization.

These optimizations collectively reduce interference, improve channel estimation accuracy, and enhance signal detection reliability

- The channel equation combining fading, spatial correlation, Doppler effect, and time-varying channel matrix of the proposed system is below.

$$H(t) = R_{rx}^{1/2} H_{real}(t) + jH_{imag}(t) R_{tx}^{1/2}$$

$H_{real}(t)$ and $H_{imag}(t)$ are time-varying real and imaginary components. R_{TX} is $N_R \times N_T$ Receive correlation matrix. Bit Error Rate (BER) performance of a Massive MIMO system with different modulation under different system configurations and SNR conditions are analyzed, and results are plotted.

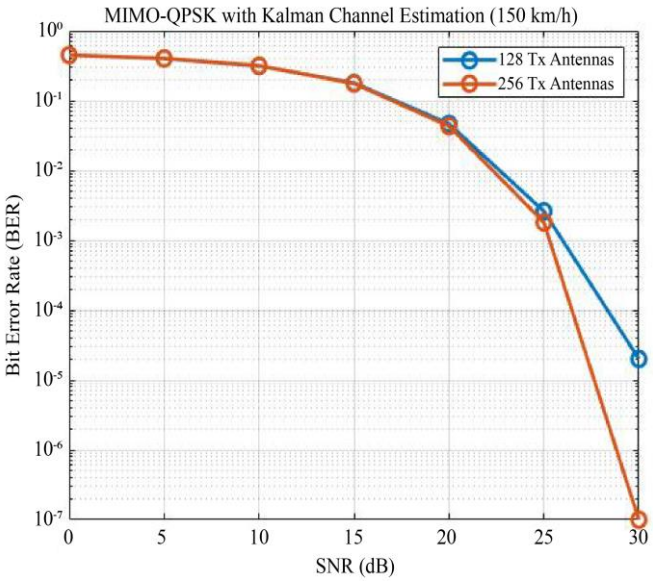

Fig. 14 BER performance for 150 km /hr speed of HST (QPSK)

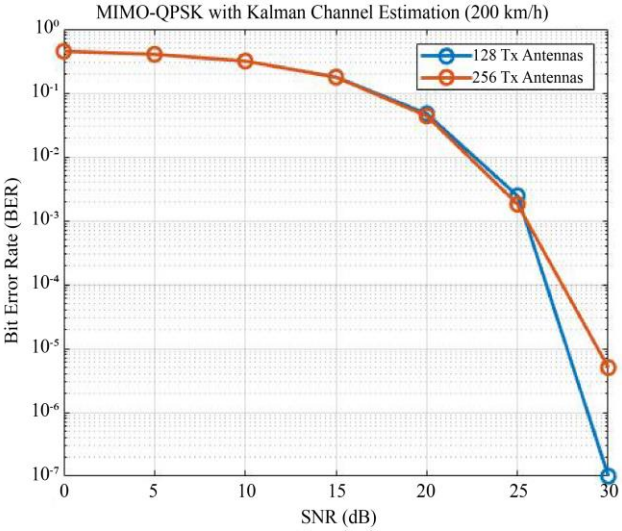

Fig. 15 BER performance for 200 km /hr speed of HST (QPSK)

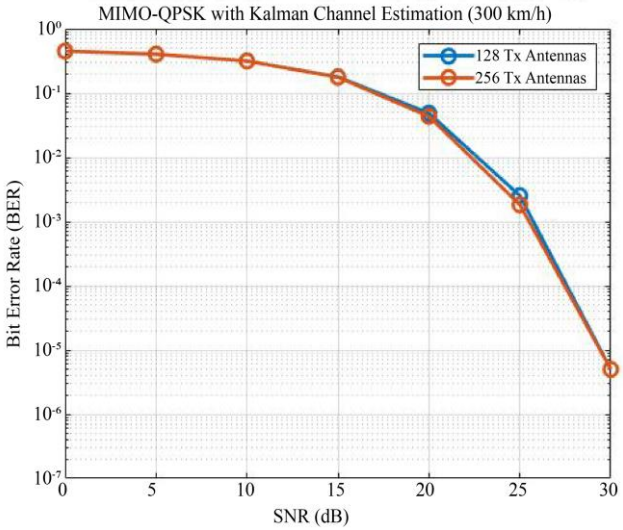

Fig. 16 BER performance for 300 km /hr speed of HST (QPSK)

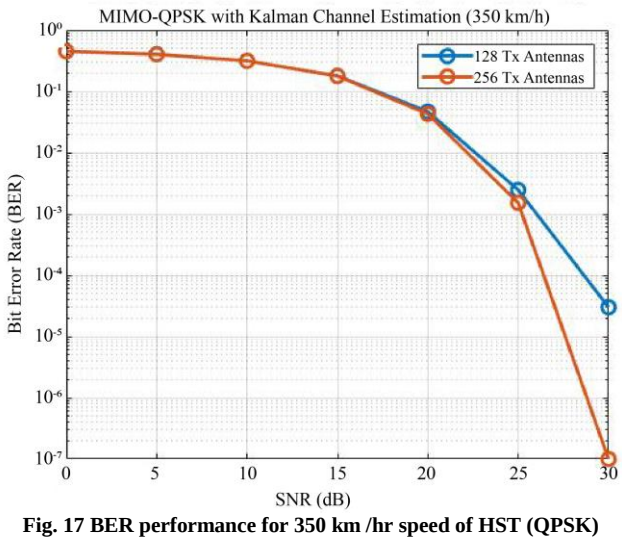

Fig. 17 BER performance for 350 km /hr speed of HST (QPSK)

Table 9. Values of parameters used in the simulation

S No.	Parameter	Value
1	No. of BS Tx antenna	128,256
2	No. of Rx antenna per user	32
3	No. of users considered	10
4	Train speed (Km/h)	150,200,300,350
5	Detection method used	MMSE
6	Signal Modulation scheme	QPSK
7	Signal carrier frequency	28 GHz
8	Channel type	Scattering
9	Precoding	Hybrid (MRT +ZF)
10	Channel estimation method	Kalman filtering
11	Doppler shift applied	Yes
12	SNR	0 dB to 30 dB

The results obtained are compared in Table 10, as shown below.

Table 10. Comparison of BER for different speed of train, TX antenna and different value of SNR

Speed of train (Km/hr)	No. of Tx antennas	BER at 15 dB SNR	BER at 25 dB SNR	BER at 30 dB SNR
150	128	0.17542	0.00260	2e-05
	256	0.17542	0.00180	1e-07
200	128	0.17543	0.00244	1e-07
	256	0.17543	0.00180	5e-06
300	128	0.17607	0.00252	5e-06
	256	0.17607	0.00182	5e-06
350	128	0.17713	0.00246	3e-05
	256	0.17713	0.00151	1e-07

The plot of BER derived for SNR ranges from 0 to 30 dB for 128 and 256 Tx antennas and different speeds of trains. As we increase Tx antennas from 128 to 256, BER reduces for 25dB SNR and above. But remains constant for 15dB SNR. Overall, we can observe that BER increases as the train's speed increases for 15 dB SNR.

Above 25 dB SNR, BER is independent of the train's speed. This proposed Massive MIMO system with channel estimation by Kalman filtering is reliable for implementation in high-speed train scenarios because its BER values are reliable above 25 dB SNR for high mobility scenarios.

6. Validation of Results with other Research Work

Achievable Ergodic rate in Bits/S/Hz is obtained for MF and MMSE receivers as mentioned in Section II. Results obtained in the plot of Figure 2 are validated with other research work.

Under the Rayleigh fading channel, expressions on the achievable rate for MF and MMSE precoding schemes are obtained[12]. Results are validated by comparing my results with the results obtained in [12].

- MF Receiver - Achievable rate (bits/S/Hz) in my work for 100 BS antennas is 28 bits/S/Hz, while in the cited research work, it is 38 bits/S/Hz.

- MMSE Receiver - Achievable rate (bits/S/Hz) in my work for 100 BS antennas is 45 bits/S/Hz, while in the cited research work, it is 80 bits/S/Hz.

The variation in obtained results is due to the variation in parameter values in both research works, such as transmit SNR, value of inter-cell interference, number of cells in a cluster, and consideration of different noise channels in the above scenario. BER vs SNR results obtained in the previous section are comparable with [24] of Massive MIMO application in High-Speed Train. BER values obtained for 15 dB, 25 dB and 30 dB SNR for high mobility scenarios are better in this work.

7. Conclusion and Future Research Scope

The high mobility of wireless communication terminals imposes many challenges on the modeling, design, analysis, and evaluation of 5G communication systems. In this paper, initially, achievable data rates for MF and MMSE receivers are derived for different numbers of BS antennas. From the

plot of Figure 2, it is concluded that as the number of antennae increases, the achievable rate also increases, and accordingly, we can select how many antennas are required to achieve the required achievable rate. From the comparison of achievable rate with MF and MMSE detection, we can observe that by using the same number of base station antenna, we can achieve a higher ergodic achievable rate with MMSE detection compared to MF detection. From Figure 4, It is observed that as we increase BS antennas, the Doppler spread decreases. Increasing the speed of high-speed trains also increases Doppler's spread. So, massive MIMO significantly decreases Doppler spread, a major parameter affecting the high data rate of broadband service in high-speed trains. Figure 12 shows that for 256 BS antennas at the transmitter, a narrow radiation beam can be formed, and thus, inter, beam interference can be reduced significantly. The new massive MIMO system is designed with a Kalman filter for channel estimation, and the results obtained are better compared to the cited reputed journal research paper. The BER versus SNR plot is obtained as shown in Table 10 for QPSK modulation and different speeds of High-speed trains. i.e. 150 km/h, 200 km/h, 300 km/h and 350 km/h. Overall, we can observe that BER increases as the train's speed increases by 15 dB SNR. Above 25 dB SNR, BER is independent of the train's speed. BER decreases as we increase the Tx antenna of the Massive MIMO system. Overall, For reliable and secure high data rate wireless communication onboard the high-speed train, a massive MIMO system with the proposed implementation shown in block diagram Figure 13 can be a key role player. Still, many areas in this field need to be worked on, as shown below.

Opportunities for future research scope can be pointed out below.

- Channel estimation errors occur due to high mobility scenarios, causing very little coherence time to estimate the channel [13].
- Due to the high speed scenario, Carrier Frequency Offset occurs due to a mismatch between transmitter and receiver frequency due to the Doppler effect, which degrades system performance[14, 5].
- A highly time-varying channel causes cross-talk due to the dominant Doppler shift [15].
- In high-speed train scenarios with double selective fading, the change of channel occurs inside one OFDM symbol and, destroys the orthogonality among subcarriers and introduces ICI also, well-sealed train carriages introduce severe penetration loss of the wireless signals [16,19].
- Parameters like directional and Omni directional antennas, the Power Delay Profile (PDP), Root Mean Square (RMS) delay spread, and small-scale PDP for both LOS and NLOS environments to be analyzed for High mobility scenarios [20-23].

References

[1] Hien Quoc Ngo, Erik G. Larsson, and Thomas L. Marzetta, "Energy and Spectral Efficiency of Very Large Multiuser MIMO Systems," *IEEE Transactions on Communications*, vol. 61, no. 4, pp. 1436-1449, 2013. [CrossRef] [Google Scholar] [Publisher Link]

[2] Jingxian Wu, and Pingzhi Fan, "A Survey on High Mobility Wireless Communications: Challenges, Opportunities and Solutions," *IEEE Access*, vol. 4, pp. 450-476, 2016. [CrossRef] [Google Scholar] [Publisher Link]

[3] Ana Gonzalez-Plaza et al., "5G Communications in High Speed and Metropolitan Railways," *11th European Conference on Antennas and Propagation*, Paris, France, pp. 658-660, 2017. [CrossRef] [Google Scholar] [Publisher Link]

[4] Yu Liu, Cheng-Xiang Wang, and Jie Huang, "Recent Developments and Future Challenges in Channel Measurements and Models for 5G and Beyond High-Speed Train Communication Systems," *IEEE Communications Magazine*, vol. 57, no. 9, pp. 50-56, 2019. [CrossRef] [Google Scholar] [Publisher Link]

[5] Jiaxun Lu et al., "Location-Aware ICI Reduction in MIMO-OFDM Downlinks for High-Speed Railway Communication Systems," *IEEE Transactions on Vehicular Technology*, vol. 67, no. 4, pp. 2958-2972, 2018. [CrossRef] [Google Scholar] [Publisher Link]

[6] Jakob Hoydis, Stephan Ten Brink, and M´erouane Debbah, "Massive MIMO in the UL/DL of Cellular Networks: How Many Antennas Do We Need?," *IEEE Journal on Selected Areas in Communications*, vol. 31, no. 2, pp. 160-171, 2013. [CrossRef] [Google Scholar] [Publisher Link]

[7] Wei Guo et al., "High-Mobility Wideband Massive MIMO Communications: Doppler Compensation, Analysis and Scaling Laws," *IEEE Transactions on Wireless Communications*, vol. 18, no. 6, pp. 3177-3191, 2019. [CrossRef] [Google Scholar] [Publisher Link]

[8] Andreas F. Molisch et al., "Hybrid Beamforming for Massive MIMO: A Survey," *IEEE Communications Magazine*, vol. 55, no. 9, pp. 134-141, 2017. [CrossRef] [Google Scholar] [Publisher Link]

[9] Zheda Li, Shengqian Han, and Andreas F. Molisch, "Hybrid Beamforming Design for Millimeter-Wave Multi-User Massive MIMO Downlink," *IEEE International Conference on Communications*, Kuala Lumpur, Malaysia, pp. 1-6, 2016. [CrossRef] [Google Scholar] [Publisher Link]

[10] K. Deepthi et al., "Massive MIMO Hybrid Beamforming," *5th International Conference for Emerging Technology*, Belgaum, India, pp. 1-5, 2024. [CrossRef] [Google Scholar] [Publisher Link]

[11] Anjali Baliyan, and Mohd. Gulamn Siddiqui, "Beam Forming Techniques in MIMO Antenna: A Review," *International Conference on Sustainable Emerging Innovations in Engineering and Technology*, Ghaziabad, India, pp. 470-474, 2023. [CrossRef] [Google Scholar] [Publisher Link]

[12] Weiqiang Tan et al., "Multiuser Precoding Scheme and Achievable Rate Analysis for Massive MIMO System," *EURASIP Journal on Wireless Communications and Networking*, vol. 208, pp. 1-12, 2018. [CrossRef] [Google Scholar] [Publisher Link]

[13] Jiakang Zheng et al., "Cell-Free Massive MIMO-OFDM for High-Speed Train Communications," *IEEE Journal on Selected Areas in Communications*, vol. 40, no. 10, pp. 2823-2839, 2022. [CrossRef] [Google Scholar] [Publisher Link]

[14] Jigang Cao et al., "Position-Aware Uplink Beamwidth Adjustment Scheme of Massive MIMO for High-Speed Railway Communications," *IEEE 11th International Conference on Communication Software and Networks*, Chongqing, China, pp. 303-308, 2019. [CrossRef] [Google Scholar] [Publisher Link]

[15] Selvi Lukman et al., "Path Loss Modelling for High-Speed Rail in 5G Communication System," *International Journal of Technology*, vol. 13, no. 4, pp. 1-12, 2022. [CrossRef] [Google Scholar] [Publisher Link]

[16] Majin Rachael Nnagana et al., "Massive MIMO for High Speed Train Communication Systems," *AU eJournal of Interdisciplinary Research*, vol. 4, no. 2, pp. 1-16, 2019. [Google Scholar] [Publisher Link]

[17] Z.A. Shamsan, "Statistical Analysis of 5G Channel Propagation using MIMO and Massive MIMO Technologies," *Engineering, Technology & Applied Science Research*, vol. 11, no. 4, pp. 7417-7423, 2021. [CrossRef] [Google Scholar] [Publisher Link]

[18] A.A. Alzamil, "Assessment of Uplink Massive MIMO in Scattering Environment," *Engineering, Technology & Applied Science Research*, vol. 10, no. 5, pp. 6290-6293, 2020. [CrossRef] [Google Scholar] [Publisher Link]

[19] Jalal Rachad, Ridha Nasri, and Laurent Decreusefond, "A 3D Beamforming Scheme Based on the Spatial Distribution of User Locations," *IEEE 30th Annual International Symposium on Personal, Indoor and Mobile Radio Communications*, Istanbul, Turkey, pp. 1-7, 2019. [CrossRef] [Google Scholar] [Publisher Link]

[20] Yang Liu et al., "Joint Beam Selection and Precoding Based on Differential Evolution for Millimeter-Wave Massive MIMO Systems," *IEEE International Conference on Acoustics, Speech and Signal Processing*, Singapore, pp. 5318-5322, 2022. [CrossRef] [Google Scholar] [Publisher Link]

[21] Yating Hu et al., "Joint Beamforming and Power Allocation Design for Stacked Intelligent Metasurfaces-Aided Cell-Free Massive MIMO Systems," *IEEE Transactions on Vehicular Technology*, pp. 1-6, 2024. [CrossRef] [Google Scholar] [Publisher Link]

[22] Yuwei Zhang et al., "Positioning-Assisted 3D Beamforming Systems and Their Outage Analysis," *IEEE/CIC International Conference on Communications in China*, Hangzhou, China, pp. 72-77, 2024. [CrossRef] [Google Scholar] [Publisher Link]

[23] Grigoriy Fokin, "Location-Aware Spatial Selection with Beam Shape and Width Control in 5G mm Wave UDN," *IEEE International Black Sea Conference on Communications and Networking*, Tbilisi, Georgia, pp. 72-77, 2024. [CrossRef] [Google Scholar] [Publisher Link]

[24] Yu Fu et al., "BER Performance of Spatial Modulation Systems under a Non-Stationary Massive MIMO Channel Model," *IEEE Access*, vol. 8, pp. 44547-44558, 2020. [CrossRef] [Google Scholar] [Publisher Link]